Predictive functional control for the temperature control of a chemical batch reactor

Hanachi Bouhenchir, Michel Cabassud, Marie-Véronique Le Lann

Predictive functional control for the temperature control of a chemical batch reactor

H. Bouhenchir [a,*], M. Cabassud [b], M.V. Le Lann [c]

[a] *NSERC Design Engineering Chair, Process Integration in the Pulp & Paper Industry, Chemical Engineering Department, Ecole Polytechnique de Montreal, Qc, Canada*
[b] *Laboratoire de Génie Chimique (UMR 5503, CNRS/INPT/UPS), Toulouse, France*
[c] *Département de Génie Electrique et Informatique, INSA, Toulouse, France*

Abstract

A predictive functional control (PFC) technique is applied to the temperature control of a pilot-plant batch reactor equipped with a mono-fluid heating/cooling system. A cascade control structure has been implemented according to the process sub-units reactor and heating/cooling system. Hereby differences in the sub-units dynamics are taken into consideration. PFC technique is described and its main differences with a standard model predictive control (MPC) technique are discussed. To evaluate its robustness, PFC has been applied to the temperature control of an exothermic chemical reaction. Experimental results show that PFC enables a precise tracking of the set-point temperature and that the PFC performances are mainly determined by its internal dynamic process model. Finally, results show the performance of the cascade control structure to handle different dynamics of the heating/cooling system.

Keywords: Predictive functional control; Model predictive control; Cascade control; Batch reactor; Temperature control; Mono-fluid system

1. Introduction

A large number of industrial processes such as the production of polymers, fine chemicals and pharmaceuticals for which continuous production is not feasible or economically attractive, are operated batchwise. In many cases this mode of operation is used to manufacture a variety of products that involve significantly different characteristics such as the conversion time, heat of the reaction, etc. Control of such type of reactors is quite often difficult to achieve (Juba & Hamer, 1986) due to their flexible and multipurpose utilization (different operating configurations and use for different productions). To guarantee batch-to-batch reproducibility and improve yield and selectivity, automation of batch reactors must be widely increased. Due to the complexity of the reaction mixture and the difficulties to perform on-line composition measurements, control of batch and fed-batch reactors is essentially a problem of temperature control (Friedrich & Perne, 1995). Batch and fed-batch reactors require good temperature control due to the existence of heat-sensitive chemical reactants and/or products and also to the dependency of reaction rate on temperature.

The temperature profile in batch reactors usually follows three-stages (Bouhenchir, Cabassud, Le Lann, & Casamatta, 2000; Preuß, Le Lann, & Anne-Archard, 2000; Xaumier, Le Lann, Cabassud, & Casamatta, 2002): (i) heating of the reaction mixture until the desired reaction temperature, (ii) maintenance of the system at this temperature and (iii) cooling stage in order to minimize the formation of by-products. Any controller used to control the reactor must be able to take into account these different stages.

In practice, the achievement of this task can be a real problem for conventional proportional-integral-derivative (PID) controllers due to the reduced stability margins provided for these applications (Huzmezan, Gough, & Kovac, 2002). These processes exhibit long dead time and time constant and have an integrating response due to the closed nature of the reactor. To keep the reactor temperatures within the products limits, operators typically resort to ad hoc PID controller over-

* Corresponding author. Tel.: +1 514 340 4711x3425; fax: +1 514 340 5150.
E-mail address: hanachi.bouhenchir@polymtl.ca (H. Bouhenchir).

Nomenclature

Process model

a_{phe} parameter (s)

$A_{cm,phe}$ heat transfer area between the cooled mono-fluid and the plate heat exchanger wall (m^2)

$A_{r,rw}$ heat transfer area between the reaction mixture and the reactor wall (m^2)

$A_{uf,phe}$ heat transfer area between the utility fluid and the plate heat exchanger wall (m^2)

b_{phe} parameter (h/m^3)

$C_{p_{cm}}$ specific heat of the mono-fluid flowing inside the plate heat exchanger (kJ/kg/K)

$C_{p_{er}}$ specific heat of the mono-fluid flowing inside the electrical resistance (kJ/kg/K)

C_{p_f} specific heat of the liquid reactant feed (kJ/kg/K)

C_{p_j} specific heat of the mono-fluid flowing inside the jacket reactor (kJ/kg/K)

$C_{p_{pw}}$ specific heat of the plate heat exchanger wall (kJ/kg/K)

C_{p_r} specific heat of the reaction mixture (kJ/kg/K)

$C_{p_{uf}}$ specific heat of the utility fluid (kJ/kg/K)

F_{cm} mono-fluid flow rate through the plate heat exchanger (m^3/s)

F_{er} mono-fluid flow rate through the electrical resistance (m^3/s)

F_f liquid reactant feed flow rate (m^3/s)

F_j mono-fluid flow rate through the jacket reactor (m^3/s)

F_{uf} utility fluid flow rate (m^3/s)

G_{er} steady-state gain of the electrical resistance (s K/kJ)

G_f steady-state liquid reactant feed gain

G_q steady-state heat released gain (s K/kJ)

$G_{r,m}$ steady-state reactor gain (PFCm controller)

$G_{r,s}$ steady-state reactor gain (PFCs controller) (K/kJ)

Pelec electrical power value (kJ/s)

Q_{cont} required thermal flux (kJ/s)

Q_{dis} global heat released (kJ/s)

Q_{rea} heat released rate by the chemical reaction (kJ/s)

$T_{cm\text{-}i,uf}$ inlet cooled mono-fluid temperature (K)

$T_{cm\text{-}o,uf}$ outlet cooled mono-fluid temperature (K)

T_{er} output electrical resistance temperature (K)

$T_{er,i}$ input electrical resistance temperature (K)

T_f liquid reactant feed temperature (K)

$T_{j,i}$ inlet jacket temperature (K)

$T_{j,o}$ outlet jacket temperature (K)

T_{pw} plate heat exchanger temperature (K)

T_r reaction mixture temperature (K)

$T_{uf,i}$ inlet utility fluid temperature (K)

$T_{uf,o}$ outlet utility fluid temperature (K)

$U_{cm,phe}$ heat transfer coefficient between the cooled mono-fluid and the plate heat exchanger wall ($kJ/m^2/s/K$)

$U_{r,wr}$ heat transfer coefficient between the reaction mixture and the reactor wall ($kJ/m^2/s/K$)

$U_{uf,phe}$ heat transfer coefficient between the utility fluid and the plate heat exchanger wall ($kJ/m^2/s/K$)

V_{cm} volume occupied by of the cooled mono-fluid inside the plate heat exchanger (m^3)

V_{er} volume occupied by of the mono-fluid inside the electrical resistance (m^3)

V_j volume occupied by the mono-fluid inside the jacket (m^3)

V_{pw} volume of the plate heat exchanger wall (m^3)

V_r volume occupied by the reaction mixture inside the reactor (m^3)

V_{uf} volume occupied by the utility fluid inside the plate heat exchanger (m^3)

Greek letters

$\delta(^\bullet)$ convexity parameter depends on the mono-fluid flow-rate

ρ_{cm} density of cooled mono-fluid (kg/m^3)

ρ_{er} density of mono-fluid inside the electrical resistance (kg/m^3)

ρ_{pw} density of plate heat exchanger wall (kg/m^3)

ρ_r density of reaction mixture (kg/m^3)

ρ_{uf} density of utility fluid (kg/m^3)

τ_{er} time constant of the electrical resistance (s)

$\tau_{phe}(^\bullet)$ time constant of the plate heat exchanger (s)

τ_r time constant of the reactor (s)

Process control

C set-point

e error

e_p predicted error

H_c coincidence point expressed on number of sampling time

$H_{c,c}$ coincidence point for PFCc controller

$H_{c,er}$ coincidence point for PFCh controller

$H_{c,g}$ coincidence point for PFCg controller

$H_{c1,m}$ first coincidence point for PFCm controller

$H_{c2,m}$ second coincidence point for PFCm controller

$H_{c1,s}$ first coincidence point for PFCs controller

$H_{c2,s}$ second coincidence point for PFCs controller

H_p prediction horizon

J objective function

Δm model prediction increment

n_B number of basis functions

p laplace operator

Δp process prediction increment

$Q_{max,cw}$ maximal thermal flux of the cold water (kJ/s)

$Q_{max,er}$ maximal thermal flux of the electrical resistance (kJ/s)

$Q_{max,gw}$ maximal thermal flux of the ethylene glycol/water (kJ/s)

$Q_{min,cw}$ minimal thermal flux of the cold water (kJ/s)

$Q_{min,er}$ minimal thermal flux of the electrical resistance (kJ/s)

$Q_{min,gw}$	minimal thermal flux of the ethylene glycol/water (kJ/s)
$T_{d,set}$	docking set-point temperature (K)
$T_{j,set}$	jacket set-point temperature (K)
$T_{r,set}$	reactor set-point temperature (K)
TRBF	95% closed loop response time (s)
$TRBF_c$	95% closed loop response time (s) for PFCc controller
$TRBF_{er}$	95% closed loop response time (s) for PFCh controller
$TRBF_g$	95% closed loop response time (s) for PFCg controller
$TRBF_r$	95% closed loop response time (s) for PFCm and PFCs controllers
ΔT	sampling period (s)
ΔT_0	sampling period for control level "0" (s)
ΔT_1	sampling period for control level "1" (s)
u	manipulated variable
U_{Bk}	basis function
y_m	model output
$y_{m,fo}$	forced model output
$y_{m,fr}$	free model output
y_p	process output
$\hat{y}_p$	predicted process output
y_r	reference trajectory

Greek letters

$\mu_k(\bullet)$	weighting factor
λ	desired speed of the reference trajectory tracking

ride schemes and slow temperature set-point ramp rates in the batch stages (heating and/or cooling stages) to deal with the poor temperature control achieved with a PID controller (Huzmezan et al., 2002). Advanced methods for PID-tuning such as a PID feedback control with dynamic compensation for process dead time (Peebles, Hunter, & Corripio, 1994) or PID controller using pre-filtered Auto-Regressive with eXternal input (ARX) estimation (Rivera & Gaikwad, 1996) can solve this problem. Nevertheless, future set-point changes still remain unforeseeable to the controller and its reaction occurs only after the change has already taken place (Preuß, Le Lann, Cabassud, Richalet, & Casamatta, 1998). Thus, the quality of a PID-control system remains unsatisfactory even with such improvements.

The elaboration of robust and efficient controllers, such as model predictive controllers (Le Lann, Cabassud, & Casamatta, 1995; Qin & Badgwell, 1996) can considerably improve the thermal control of such reactors. Model predictive control (MPC) is a generic term widely used for a class of computer control algorithms that use an explicit process model to predict the future response of a plant (Badgwell & Qin, 2001). At each control interval, a MPC algorithm determines a sequence of manipulated variable adjustments that optimize the future plant behavior. The first value in the optimal sequence is then sent into the plant and the entire optimization is repeated at subsequent control intervals.

During the last decade, a plethora of papers and applications of MPC algorithms have appeared in the open literature. The success of MPC technology as a process control paradigm can be attributed to three important factors (Badgwell & Qin, 2001). First and foremost is the incorporation of an explicit process model into the control computation. This allows the controller, in principle, to deal directly with all significant features of the process dynamics. Secondly, MPC controller algorithm considers the plant behavior over a future horizon in time. This means that the effects of feedforward and feedback disturbances on the plant can be anticipated and removed, allowing the controller to drive the plant more closely along a desired features trajectory. Finally, MPC controllers consider process input, state and output constraints directly in the control calculation. This means that constraint violations are far less likely to happen, which results in a tighter control of the process.

A MPC control strategy consists of basically two main parts: firstly, an explicit process model (based on thermal and/or mass balances), allows the controller to deal with all significant features of the process dynamics, and secondly, an optimization problem. By using different types of models and different optimization problems, a large variety of MPC control strategies can be obtained.

To achieve the control of batch or fed-batch reactors, various MPC schemes were applied by a number of researchers. When studying a polymerization batch reactor, (Defaye, Régnier, Chabanon, Caralp, & Vidal, 1993) used a Model Based Predictive Control algorithm (MBPC) associated to an adaptive algorithm using the recursive least squares (RLS) method. As a first step, they compared the performances of the MBPC algorithm to a classical PID controller. Later, the results obtained with an adaptive MBPC controller were contrasted with those produced with the non-adaptive version of the MBPC for the thermal control of a moderately exothermic copolymerization reaction. They reached the conclusion that the application of MBPC controller in its adaptive version gives a better thermal control of semi-batch polymerization reactors. Özkan, Hapoglu, and Alpbaz (1998) have experimentally and theoretically studied a Generalized Predictive Control (GPC) algorithm for the thermal control of a free radical styrene polymerization in a cooling jacketed mixing batch reactor. The optimal temperature policies were obtained at different initiator concentrations by applying the optimal control theory. The GPC control method was based on the ARIMAX (Auto-Regressive Integrated Moving-Average with eXogenous Input) model. In this case also, the GPC performances were compared to a classical PID controller for two optimal temperature trajectories. The results showed that the GPC performed better. Lee, Chin, and Lee (1999) presented a new technique for the thermal control of batch reactors called Batch-MPC. This technique is based on a time-varying linear system model and it utilizes not only the incoming measurements from the ongoing batch, but also the information stored from the past batches. This particular feature is shown to be essential for achieving effective tracking control performance despite model errors and disturbances. In a series of experi-

ments performed on a bench-scale batch reactor system, the technique was found to deliver satisfactory tracking performances overcoming a large amount of model uncertainty and various process disturbances. Bouhenchir, Cabassud, Le Lann, and Casamatta, (2001) presented experimental and simulation studies for the temperature control of industrial batch reactors (16, 65 and 160 l) equipped with a multi-fluid heating/cooling systems. They used adaptive GPC with double model references [GPC-MR: one model reference on the input and one on the output] and supervision strategy based on the limits thermal flux analysis. Experimental and theoretical results demonstrated the feasibility of such technique. A novel tuning approach of the GPC algorithm has been proposed by (Rodrigues, Toledo, & Maciel Filho, 2002) in both adaptive and non-adaptive configurations for a fed-batch penicillin process using the complete factorial design method. It was found that the controller stabilizes the dissolved oxygen concentration through agitation. This approach provides the optimal set of parameters by estimating the effect of the design parameters on the integral of the absolute error between the controlled variable and the set point. They found that the performances of such controllers are better than those obtained with a classical PID controller or a dynamic model control (DMC) algorithm.

Even though the different MPC approaches presented above gave satisfactory results for batch reactor control than conventional PID controllers, they also involve the resolution of a quadratic problem (QP). The computational burden associated with solving an on-line QP can be heavy and may require a standalone computer. In the last decade a predictive functional control (PFC) technique has been pioneered (Richalet, 1993). The advantage of PFC compared to the different MPC configurations is its flexibility to transform a QP problem into a square system of equations, which allows for an easier implementation in practice. Also PFC is distinct from other MPC implementations in several ways: the SISO version, uses reference trajectories, coincidence points and can be applied to the control of a linear or non-linear process without need of model linearization (Badgwell & Qin, 2001). PFC is very open and can integrate a number of concepts resulting from other approaches. It can be implemented in simple industrial automats but also in numerical systems of centralized control (NSCC) or industrial PCs (Richalet, Lavilelle, & Mallet, 2004). The PFC technique handles systems with varying dynamics, with or without integrator, with stable or unstable open loop, with or without dead time, and, generally systems that are difficult to control with a classical PID. The attractive features of PFC are:

- Natural concepts, therefore accessible to any technical staff.
- Parameters related to the performance: specification parameters and not tuning parameters.
- Methodologies allowing extension of its principles to a wide field of process control applications.

The objective of this work is to apply the PFC technique to the temperature control of a chemical batch jacketed reactor equipped with a mono-fluid heating/cooling system. This algorithm proved to be highly robust and precise in different studies (Primucci & Basualdo, 2002). The paper is organized as follows. In Section 2, a mathematical calculation of a PFC design is given and explained the principle of such technique. A description of a batch scale reactor and its heating/cooling system used for experiments is given in Section 3. Section 4 presents the cascaded PFC controllers developed, form the reactor, its jacket and the heating/cooling system modeling. In Section 5, experimental results obtained on the pilot-plant are given to illustrate the performance of this technique. Conclusions are given in Section 6.

2. Mathematical calculation for PFC design

PFC basically consists of the following elements:

- An internal model for the on-line prediction of the future system's behavior. This model is embedded in the controller.
- A reference trajectory $y_r(n)$ which describes the smooth transition of the process output from its current value to the future set-point profile $C(n)$ within a prediction horizon H_p that corresponds to the end of the coincidence horizon H_c. This trajectory can be interpreted as the desired behavior of the closed loop system.
- An objective function $J(u,e)$ as a "Quadratic" function of the future controller error $e(n)$ between the reference trajectory and the predicted output over a coincidence horizon $[H_1,H_c]$.
- A compensation for modeling errors.

As depicted in Fig. 1, by minimizing the objective function, an optimal profile of the future values of the manipulated variable

$$u_{opt}^{T} = [u(n+1), u(n+2), ..., u(n+H_c)] \quad (1)$$

is calculated for the coincidence horizon that guides the predicted process output as close as possible to the reference trajectory. This calculation is based on:

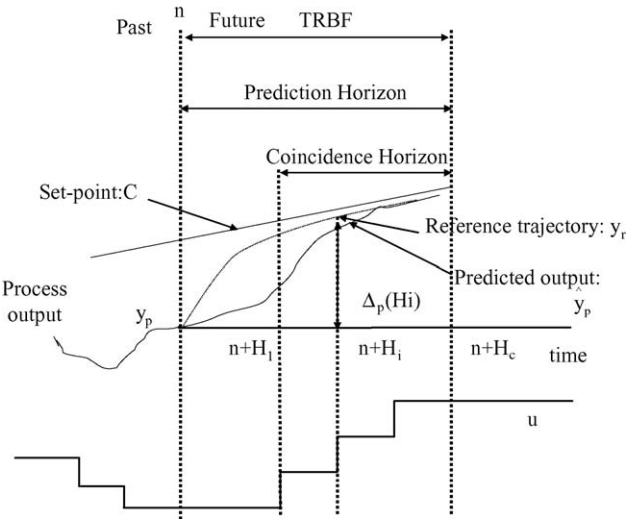

Fig. 1. Principle of PFC.

- the future values of the process output predicted by the internal dynamic model

$$\hat{y}_{\mathrm{p}}^{\mathrm{T}} = [\hat{y}_{\mathrm{p}}(n+H_1), \hat{y}_{\mathrm{p}}(n+H_2), ..., \hat{y}_{\mathrm{p}}(n+H_{\mathrm{c}})] \quad (2)$$

- a given set-point profile which corresponds to the reference trajectory

$$\hat{y}_{\mathrm{r}}^{\mathrm{T}} = [y_{\mathrm{r}}(n+H_1), y_{\mathrm{r}}(n+H_2), ..., y_{\mathrm{r}}(n+H_{\mathrm{c}})] \quad (3)$$

- the future controller error

$$e^{\mathrm{T}} = [\Delta y(n+H_1), \Delta y(n+H_2), ..., \Delta y(n+H_{\mathrm{c}})] \quad (4)$$

where

$$\Delta y(n+j) = \left| y_{\mathrm{r}}(n+j) - \hat{y}_{\mathrm{p}}(n+j) \right| \quad (5)$$

and optionally

- a prediction of the model-error

$$e_{\mathrm{p}}^{\mathrm{T}} = [e_{\mathrm{p}}(n+1), ..., e_{\mathrm{p}}(n+H_{\mathrm{c}})]. \quad (6)$$

The minimization of the objective function leads to the optimal profile of the manipulated variable. Only its first element $u_{\mathrm{opt}}(n+1)$ is applied to the process. After a one step shift of the data arrays the calculation is repeated at the next period.

The principal characteristic of the PFC technique is the representation of the manipulated variable as a sum of a set of pre-determined basis functions u_{Bk}

$$u(n+i) = \sum_{k=1}^{n_{\mathrm{B}}} \mu_k(n) u_{\mathrm{Bk}}(i). \quad (7)$$

Minimizing the objective function requires therefore less calculation because only the optimal set of weighting factors μ_k has to be found. The choice of the basis functions is a tuning parameter of PFC. Some examples of basis functions are shown in Fig. 2. In general there are no limits on the choice of the basis functions. They might be polynomial, sine or exponential functions. They are chosen according to the set-point profile and the expected disturbances. It can be shown that in the nominal case (no model mismatch) there will be no lag-error on any set point if the basis functions are chosen properly (Richalet, 1993). Usually the set-point profile and the disturbances can be approximated by polynomials. In this case the basis functions can be expressed by series:

$$u_{\mathrm{Bk}}(i) = i^{k-1} \quad \forall k. \quad (8)$$

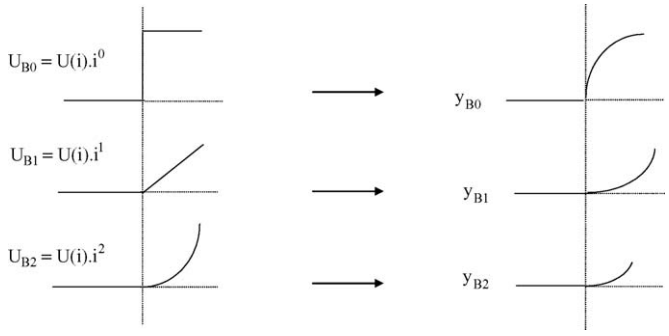

Fig. 2. Examples of base functions.

Let $\Delta p(H_i)$ be the increment between the actual process output $y_{\mathrm{p}}(n)$ and the reference trajectory $y_{\mathrm{r}}(n)$ at the future point of coincidence H_i between H_1 and H_{c}:

$$\Delta p(H_i) = y_{\mathrm{r}}(n+H_i) - y_{\mathrm{p}}(n) \quad (9)$$

where

$$y_{\mathrm{r}}(n+H_i) = C(n+H_i) - \lambda^{H_i}[C(n) - y_{\mathrm{p}}(n)] \quad (10)$$

is a first order exponential reference trajectory and $\lambda = \exp(-3\Delta t/\mathrm{TRBF})$ is the parameter that specifies the desired tracking speed. Thus, for a given constant set point the increment can be transformed with Eqs. (9) and (10) into

$$\Delta p(H_i) = [C(n) - y_{\mathrm{p}}(n)](1 - \lambda^{H_i}). \quad (11)$$

Since the control objective is to make the model output match the reference trajectory. For one coincidence point H_i, the PFC control law is given by the following equation:

$$y_{\mathrm{r}}(n+H_i) - \hat{y}_{\mathrm{p}}(n+H_i) = 0. \quad (12)$$

The model output can be considered as the superposition of the zero-state response (forced response) and the zero-input response (free response):

$$\hat{y}_{\mathrm{p}}(n+H_i) = y_{\mathrm{m,fo}}(n+H_i) + y_{\mathrm{m,fr}}(n+H_i) + y_{\mathrm{p}}(n) - y_{\mathrm{m}}(n). \quad (13)$$

Therefore, the following basic control law for PFC can be derived:

$$\Delta p(H_i) = \Delta m(H_i) \quad \text{where} \quad \Delta p(H_i) = [C(n) - y_{\mathrm{p}}(n)](1 - \lambda^{H_i}),$$
$$\Delta m(H_i) = y_{\mathrm{m,fo}}(n+H_i) + y_{\mathrm{m,fr}}(n+H_i) - y_{\mathrm{m}}(n). \quad (14)$$

Notice that PFC control law for one coincidence point is a first order exponential reference trajectory. If more coincidence points are used, a quadratic criterion should be used

$$J = \sum_{H_i=H_1}^{H_{\mathrm{c}}} [\Delta p(H_i) - \Delta m(H_i)]^2. \quad (15)$$

For any basis function as input to a given model a base-output function can be calculated (cf. Fig. 2). In this case the forced response can be written as

$$y_{\mathrm{m,fo}}(n+i) = \sum_{k=1}^{n_{\mathrm{B}}} \mu_k(n) u_{\mathrm{Bk}}(i) \quad (16)$$

thus Eqs. (14) and (15) can be transformed respectively to

$$\Delta p(H_i) = \Delta p(H_i) \quad \text{where} \quad \Delta p(H_i) = [C(n) - y_{\mathrm{p}}(n)](1 - \lambda^{H_i}),$$
$$\Delta m(H_i) = \sum_{k=1}^{n_{\mathrm{B}}} \mu_k(n) u_{\mathrm{Bk}}(H_i) + y_{\mathrm{m,fr}}(n+H_i) - y_{\mathrm{m}}(n) \quad (17)$$

$$J = \sum_{H_i=H_1}^{H_c} \left[\Delta p(H_i) - y_{m,fr}(n+H_i) - \sum_{k=1}^{n_B} \mu_k(n) u_{Bk}(H_i) + y_m(n) \right]^2 . \quad (18)$$

Notice that the number of basis functions used n_B, forces a lower limit on the necessary number of coincidence points n_c to obtain a solution. If n_B basis functions are used then n_B coefficients μ_k must be determined from n_c equations, in this case the minimization of J can be carried out by the least squares algorithm. However, when the number of coincidence points n_c equals the number of basis functions n_B, it raises only the resolution of a square system of n_c equations and n_c unknowns coefficients μ_k (Boucher & Dumur, 1996).

3. Experimental system

A schematic diagram of the pilot plant is depicted in Fig. 3. The experimental device consists of a 1 l jacketed glass reactor, fitted with a mono-fluid heating/cooling system. The mono-fluid used in this work is a mixture of ethylene glycol and water, in a ratio of 50% in weight, with a flow rate of 1000 l h^{-1} and at a temperature which varies between −35 and 110 °C. The mono-fluid flow-rate is measured by means of two flow-meters, one installed on the main thermal loop (Flow-meter 1) and the other one on the secondary thermal loop (Flow-meter 2). The heating/cooling system uses a 2000 W electrical resistance and two plate heat-exchangers (PHE). One PHE uses cold water as an utility fluid at a temperature around 15 °C and a maximum flow rate of 1500 l h^{-1}, while the other one uses a mixture of ethylene glycol and water, in a ratio of 50% in weight, at a temperature around −10 °C and a maximum flow of 1500 l h^{-1}. Flow rates of the utility fluids are also measured. Three on–off valves allow the mono-fluid to be heated or cooled. Two other on–off valves are used to manipulate the utility fluids. A three ways air-to-open valve ensures the division of the mono-fluid in two parts during the cooling phases. A gearing pump ensures the circulation of the mono-fluid in the thermal loop at maximum flow rate of 1500 l h^{-1}.

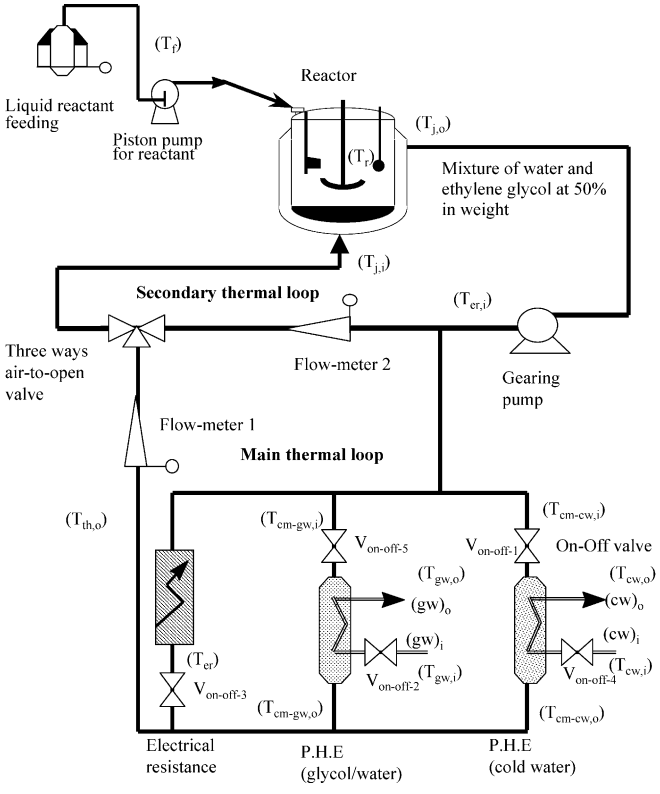

Fig. 3. Schematic of the pilot pant.

The reactor has the following physical specifications: an internal diameter of 82 mm, a wall thickness of 9 mm, an external jacket diameter of 125 mm, a jacket wall thickness of 5 mm, a maximal reactant mixture-reactor heat transfer area of 0.039 m^2 and a jacket volume of 0.15 l. A propeller rotated at 260 rpm. The reactor is operated in batch and fed-batch modes. A piston pump allows the variation of the liquid reactant flow rate from 0 to 336 cm^3 h^{-1}.

All temperatures are measured at each sampling period using PT100 platinum resistance sensors with a precision of ±0.1 °C. The feed temperature of inlet reactant is measured by a thermocouple. A computer with Analog-to-Digital (A/D) and Digital-to-Analog (D/A) converters is employed for data acquisition and the control of the experimental system. The supervision and control algorithms programs are written in Pascal 7 and are implemented on a PC in order to accomplish the different temperature control tasks.

4. PFC controllers

The control system must manipulate the inlet jacket reactor temperature ($T_{j,i}$) using the electrical resistance and the two plate heat-exchangers (PHE), to control the reaction mixture temperature (T_r). A cascade control structure using the PFC technique is implemented. Two control levels "1" and "0" are considered. Two controllers are used in the control level "1". The first one in charge of supervision, it computes the required thermal flux (Q_{cont}) to be exchanged between the mono-fluid flowing inside the jacket and the reaction mixture. The second one is devoted to compute the set-point temperature ($T_{j,set}$) which will be tracked by the inlet jacket temperature ($T_{j,i}$). In the control level "0", three slave controllers are used to control the mono-fluid temperature. One placed on the electrical resistance which computes the electrical power value and the two other on the two PHEs to compute the mono-fluid flow rate fraction dispatched to one of them.

The performances of the PFC are mainly determined by its internal process model. Process modeling and details of the different algorithms can be found in Bouhenchir (2000). In this paper only the internal dynamic models are presented. The experimental device has been divided into fourth sub-units: the reactor, the electrical resistance and the two PHE. Theses sub-units are modeled independently and presented bellow.

4.1. The reactor

The reactor can be described by the following thermal balances:

- thermal balance on the reaction mixture:

$$\rho_r C_{p_r} V_r \frac{dT_r}{dt} = UA_{r,rw}(T_{j,o} - T_r) + F_f \rho_f C_{p_f}(T_f - T_r) - Q_{rea} \quad (19)$$

- thermal balance on the mono-fluid flowing inside the jacket:

$$\rho_j C_{p_j} V_j \frac{dT_{j,o}}{dt} = UA_{r,rw}(T_r - T_{j,o}) + F_j \rho_j C_{p_j}(T_{j,i} - T_{j,o}). \quad (20)$$

Two controllers are used in the main controller loop, the first one called PFCs in charge of supervision; and the second one called PFCm devoted to compute the jacket set-point temperature used by the slave controllers.

The internal model used by the PFCs controller was derived from Eq. (19) and it is given by the following continuous system transfer function equation using the laplace transform:

$$T_r(p) = \frac{G_{r,s}}{p}(Q_{cont}(p) + Q_{dis}(p)) \quad (21)$$

where $G_{r,s} = 1/\tau_r UA_{r,rw}$ is the steady-state gain, $Q_{cont} = UA_{r,rw}(T_{j,o} - T_r)$ the thermal flux exchanged between reaction mixture and the mono-fluid flowing inside the jacket, and $Q_{dis} = F_f \rho_f C_{p_f}(T_f - T_r) - Q_{rea}$ the disturbance caused by feed reactants and the heat released by the chemical reaction. We can notice that Eq. (21) presents a pure integrating and unstable internal model. To solve this problem, decomposition principle was applied (Richalet, 1993). It allows decomposing the unstable internal model into two stable models, one having as input (Q_{cont}) "the manipulated variable" and the other one, the actual measured reactor temperature.

The internal model used by the PFCm controller was derived from Eqs. (19) and (20) and it is given by the following transfer functions using the laplace transform:

$$\frac{T_r(p)}{T_{j,i}(p)} = \frac{1}{1 + G_f\frac{k+1}{k} + \left[\left(\frac{k+1}{k}\right)\theta_r + \left(\frac{G_f+1}{k}\right)\theta_s\right] p + \frac{\theta_r\theta_s}{k}p^2},$$

$$\frac{T_r(p)}{T_f(p)} = \frac{\frac{k+1}{k}G_f\left(\frac{\theta_s}{k+1}p + 1\right)}{1 + G_f\frac{k+1}{k} + \left[\left(\frac{k+1}{k}\right)\theta_r + \left(\frac{G_f+1}{k}\right)\theta_s\right] p + \frac{\theta_r\theta_s}{k}p^2},$$

$$\frac{T_r(p)}{Q_{rea}(p)} = \frac{\frac{k+1}{k}G_q\left(\frac{\theta_s}{k+1}p + 1\right)}{1 + G_f\frac{k+1}{k} + \left[\left(\frac{k+1}{k}\right)\theta_r + \left(\frac{G_f+1}{k}\right)\theta_s\right] p + \frac{\theta_r\theta_s}{k}p^2} \quad (22)$$

where $\theta_r = (\rho_r C_{p_r} V_r / UA_{r,rw})$, $\theta_s = (\rho_j C_{p_j} V_j / UA_{r,rw})$, $G_f = \theta_r(F_f \rho_f C_{p_f} / \rho_r C_{p_r} V_r)$, $G_q = \theta_r(1/\rho_r C_{p_r} V_r)$ and $k = (\theta_s F j / V_j)$.

Evidently the reactor system is a second order process. Numerical manipulation of the denominators and numerators gives two real poles (−1.861, −0.5687) and two real zeros (−1.861, −1.861) for the second and the third transfer function. Via a pole-zero cancellation, transfer functions between T_r and T_f and between T_r and Q_{rea} become first order with a real pole at −0.5687. The transfer function relating the reactor temperature T_r to the jacket inlet temperature $T_{j,i}$, had two poles. The pole at −1.861 is far from the origin and corresponds to the fast dynamics while the pole at −0.5687 closer to the origin corresponds to the slow dynamics. Fig. 4 shows the second order step response (T_r_$T_{j,i}$_2nd) against the first order step response (T_r_$T_{j,i}$_1st), using the pole −0.5687. The two responses have the same trend and so, this pole is predominant one. Based on this, the following model was proposed to construct the PFCm controller:

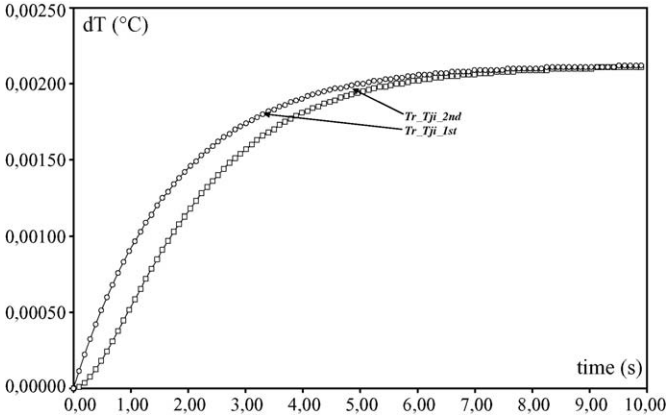

Fig. 4. Step response of the reactor temperature.

$$T_r(p) = \frac{G_{r,m}}{1 + \tau_r p}T_{j,i}(p) + \frac{G_f}{1 + \tau_r p}T_f(p) + \frac{G_q}{1 + \tau_r p}Q_{rea}(p). \quad (23)$$

The time constant τ_r was identified via simulation.

In the following paragraphs, we will substitute ($T_{j,i}$) in Eq. (23) by ($T_{j,set}$) which denotes the set-point to the inlet jacketed reactor temperature. This value will be calculated by the PFCm controller.

4.2. The electrical resistance

The dynamics of the electrical resistance can be described by the following thermal balance:

$$\rho_{er} C_{p_{er}} V_{er} \frac{d}{dt}(T_{er} - T_{er,i}) = \rho_{er} C_{p_{er}} F_{er}(T_{er,i} - T_{er}) + \text{Pelec}. \quad (24)$$

The internal model used by slave controller called PFCh is derived from Eq. (24) and it is given by the following continuous system transfer function:

$$T_{er}(p) = T_{er,i}(p) + \frac{G_{er}}{1 + \tau_{er} p}\text{Pelec}(p) \quad (25)$$

where: G_{er} and τ_{er} denotes, respectively, the steady-state gain and the time constant of the electrical resistance.

4.3. The plate heat-exchangers

The dynamics of plate heat exchangers can be described by the following equations:

- thermal balance on the mono-fluid:

$$\rho_{cm} C_{p_{cm}} V_{cm} \frac{dT_{cmo,uf}}{dt} = F_{cm}\rho_{cm} C_{p_{cm}}(T_{cmi,uf} - T_{cmo,uf}) + U_{cm,phe} A_{cm,phe}(T_{pw} - T_{cmo,uf}) \quad (26)$$

- thermal balance on the plate wall:

$$\rho_{pw} C_{p_{pw}} V_{pw} \frac{dT_{pw}}{dt} = U_{cm,phe} A_{cm,phe}(T_{cmo,uf} - T_{pw}) + U_{uf,phe} A_{uf,phe}(T_{uf,o} - T_{pw}) \quad (27)$$

- thermal balance on the utility fluid:

$$\rho_{uf} C_{p_{uf}} V_{uf} \frac{dT_{uf,o}}{dt} = F_{uf}\rho_{uf} C_{p_{uf}}(T_{uf,i} - T_{uf,o}) + U_{uf,phe} A_{uf,phe}(T_{pw} - T_{uf,o}). \quad (28)$$

From theses equations, an internal dynamic model (used by slave controller PFCc for PHE using cold water and by a slave controller PFCg for PHE using a mixture of ethylene glycol and water) is derived and it is given by the following equation:

$$T_{cmo,uf}(p) = \frac{\delta(F_{cm})}{(1 + \tau_{phe}(F_{cm})p)} T_{cmi,uf}(p) + \frac{(1 - \delta(F_{cm}))}{(1 + \tau_{phe}(F_{cm})p)} T_{uf,i}(p) \quad (29)$$

where $T_{uf,i}$ is the utility fluid temperature at the inlet of PHE used; i,uf denotes inlet utility fluid, its value equals to i,cw when the fluid is the cold water or i,gw when the fluid is the mixture of ethylene glycol and water; o,uf denotes outlet utility fluid, its value equals to o,cw when the fluid is the cold water or o,gw when the fluid is the mixture of ethylene glycol and water; $\tau_{phe}(F_{cm})$ denotes the time constant of the PHE and it is given by the following relationship: $\tau_{phe}(F_{cm}) = a_{phe} F_{cm}^{b_{phe}}$.

As it is shown in Eq. (29), the cooling process can be approximated to a first order with a time constant that depends on the mono-fluid flow-rate F_{cm} ($0 \le F_{cm} \le F_j$). Hence, when manipulating F_{cm}, we actually change the time constant of the PHE. In fact, with the flow rate as manipulated variable, an action does not modify the final steady-state but influences the speed to reach this steady-state. In other words, a parameter is controlled instead of a variable. Accordingly the control of plate heat exchanger is performed by using parametric predictive control (PPC) which is an extension of the PFC technique to control non-linear systems (Richalet, 1993). In this case PPC has to determine a value for the time constant such that the predicted response of the process tracks the reference trajectory.

Table 1
Inputs and outputs of sub-unit models

Controller	Set-point	Controlled variable	Manipulated variable
PFCs	$T_{r,set}$	T_r	Q_{cont}
PFCm	$T_{r,set}$	T_r	$T_{j,set}$
PFCh	$T_{j,set}$	$T_{j,i}$	Pelec
PFCc	$T_{j,set}$	$T_{j,i}$	(F_{cm})cw
PFCg	$T_{j,set}$	$T_{j,i}$	(F_{cm})gw

4.4. Summary of the control strategy

Table 1 shows the relation between inputs and outputs of the sub-unit models. The controlled variable is the temperature of the reaction mixture (T_r), which changes according to the required thermal flux (Q_{cont}) and the inlet temperature of the mono-fluid ($T_{j,i}$). In turn $T_{j,i}$ is determined by the electrical resistance and the PHEs. Hence $T_{j,i}$ is considered as an intermediate controlled variable linked to cascade control levels. Hereby closed loop dynamic performance is improved, particularly since the predominating time constant of reactor is significantly greater than those of the electrical resistance and PHEs (cf. Table 2). According to time constants, the sampling periods has been chosen to be 30 s for the control level "1" and 3 s for the control level "0".

According to the set-point temperature profile represented by a heating, a constant temperature and a cooling stages, the controllers PFCs and PFCm use two basis functions; a step and a ramp. As far as the control level "0" is concerned precise tracking of set-point profiles is not necessarily required (because of the much faster dynamics involved compared to the control level "1") structuring of the manipulated variables of the slaves controllers by one single basis function (the step function) is assumed to be sufficient.

As depicted in Fig. 5 the supervisor PFCs computes a required thermal flux which is compared to the limit capacities of the thermal elements ($Q_{max,er}$, $Q_{min,er}$, $Q_{max,cw}$, $Q_{min,cw}$, $Q_{max,gw}$,

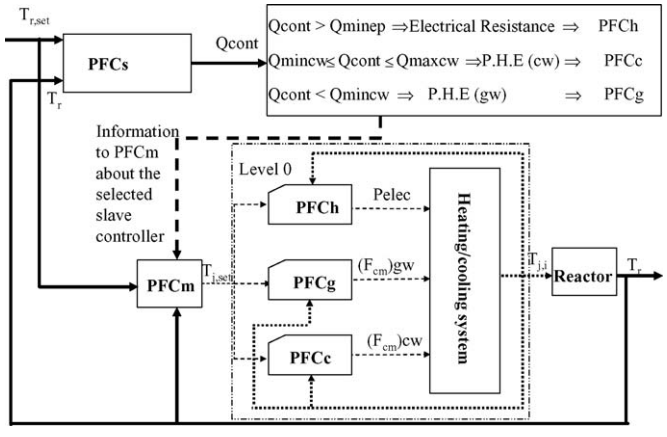

Fig. 5. PFC controllers.

Table 2
Numerical values related to the PFC controllers' parameters

$G_{r,s}$	τ_r (s)	$H_{c1,s}$	$H_{c2,s}$	$U_{B1,s}$	$U_{B2,s}$	$TRBF_r$ (s)	ΔT_1 (s)
PFCs							
1	280	2	10	1	$1+H_i$	200	30
$G_{r,m}$	$\tau_{r,m}$ (s)	$H_{c1,m}$	$H_{c2,m}$	$U_{B1,m}$	$U_{B2,m}$	$TRBF_r$ (s)	ΔT_1 (s)
PFCm							
1	280	2	10	1	$1+H_i$	200	30
G_{er} (s K/kJ)		τ_{er} (s)		$H_{c,er}$		$TRBF_{er}$ (s)	ΔT_0 (s)
PFCh							
1		20		3		30	3
a_{phe} (s)		b_{phe} (h/m^3)		$H_{c,c}$		$TRBF_c$ (s)	ΔT_0 (s)
PFCc							
31541		0.836		10		80	3
a_{phe} (s)		b_{phe} (h/m^3)		$H_{c,g}$		$TRBF_g$ (s)	ΔT_0 (s)
PFCg							
46358		−0.72		10		80	3

$Q_{min,gw}$) in order to select the adequate apparatus (Bouhenchir, 2000; Bouhenchir et al., 2000). Once the apparatus is selected, the corresponding controller from level "0" is chosen. The master controller PFCm computes the jacket set-point temperature $T_{j,set}$ for the selected controller. If PFCh is selected, the manipulated variable is the electrical power value Pelec. If PFCc (or PFCg) is selected the manipulated variable is the mono-fluid flow rate fraction value (F_{cm})cw (or (F_{cm})gw) dispatched to the PHE.

5. Experimental results and discussions

To demonstrate the good performance of the PFC technique, different experiments have been carried out on the pilot-plant reactor previously described. More details can be found in Bouhenchir (2000). In this paper, we present the experimental results obtained for the temperature control of an exothermic acid–base neutralization chemical reaction between the hydrochloric acid (HCl) and the sodium hydroxide (NaOH) to test the robustness of the control system when there dynamics changeovers, due to the heat release, during the constant set-point stage.

The reactor was fed with a solution of hydroxide sodium (NaOH/water = 57.14 g/485.71 g) at temperature of 22 °C. The set-point temperature profile is composed by: first stage: heating from 22 to 45 °C during 1500 s (0.92 °C min^{-1}); second stage: constant temperature at 45 °C during 3500 s in which solution of hydrochloric acid (HCl/water = 44.03 g/74.97 g) is fed during 2000 s; third stage: cooling from 45 to 30 °C during 1500 s (−0.6 °C min^{-1}) and fourth stage: maintain at 30 °C during 500 s. However this temperature profile is composed by an increasing ramp—maintain and decreasing ramp. In order to eliminate discontinuities resulting from change of stage, the set-point profile was filtered by a procedure called "docking procedure" which transforms the temperature profile as shown in Fig. 6. We get a softer set-point profile at any stage changeover. More details are given in the Appendix A.

5.1. Temperature control without taking account disturbances due to the exothermic reaction

In this experiment, the controllers of the master loop, PFCs and PFCm are composed by two internal dynamic models that that take into account only the heat exchanged between the reaction mixture and the mono-fluid flowing inside the jacket as described by the following equations:

- for the controller PFCs:

$$T_r(p) = \frac{G_{r,s}}{p} Q_{cont}(p) \tag{30}$$

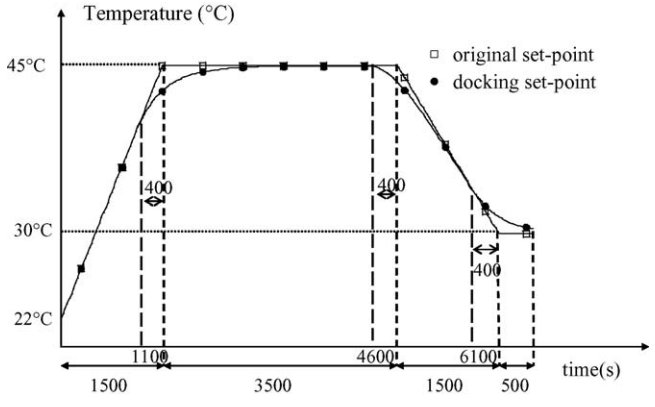

Fig. 6. Docking set-point temperature.

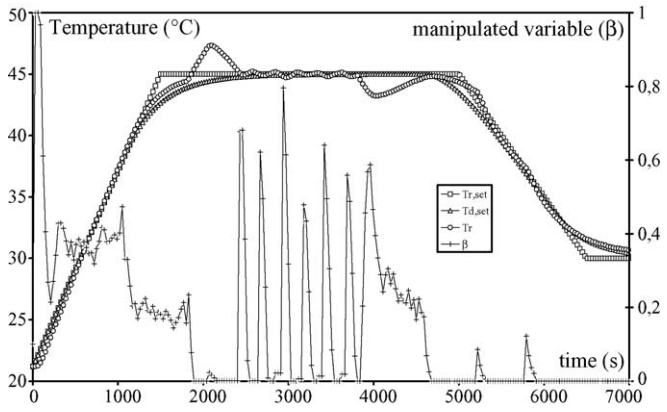

Fig. 7. Temperature and manipulated variable (model mismatch).

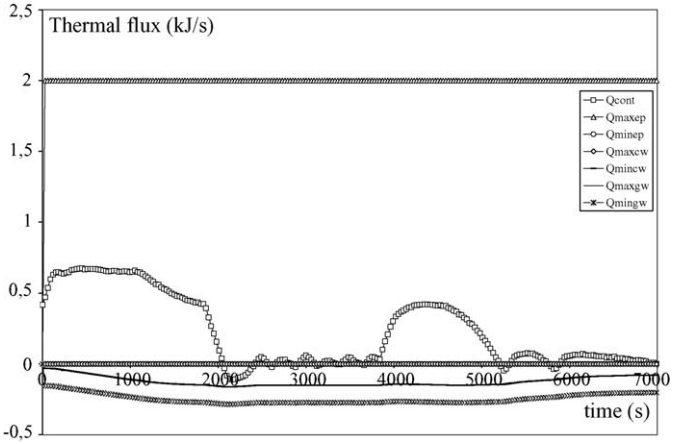

Fig. 8. Limits and required thermal flux (model mismatch).

- for the controller PFCm:

$$T_{\mathrm{r}}(p) = \frac{G_{\mathrm{r,m}}}{1+\tau_{\mathrm{r}}p} T_{\mathrm{j,set}}(p). \tag{31}$$

The solution of hydrochloric acid was fed between 1800 and 3800 s and the experimental results are presented in Figs. 7–9.

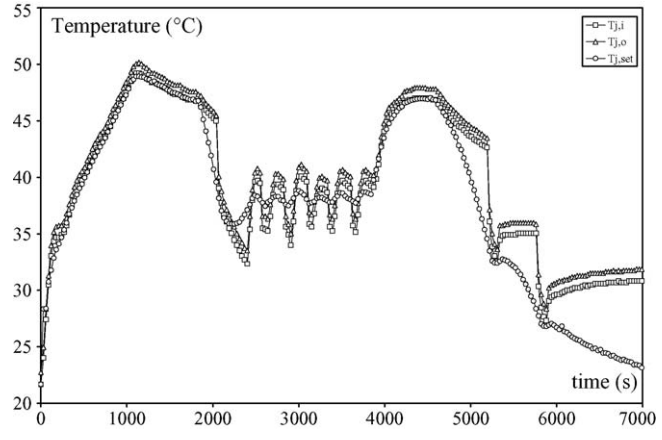

Fig. 9. Inlet, outlet and set-point jacket temperatures (model mismatch).

Fig. 7 presents the time evolution of the set point ($T_{\mathrm{r,set}}$), the adjusted set point ($T_{\mathrm{d,set}}$) and the reaction mixture (T_{r}) temperatures (left y-axis) and the manipulated variable (β) computed by the slave controllers (right y-axis). The manipulated variable (β) denotes the fraction (compared to its maximum) of the electrical power value or the mono-fluid flow rate fraction dispatched to one of the two PHE. Fig. 8 gives the time evolution of the required thermal flux (Q_{cont}) computed by PFCs and the limit thermal capacities for the electrical resistance ($Q_{\mathrm{min,er}}$, $Q_{\mathrm{max,er}}$), for the PHE using cold water ($Q_{\mathrm{min,cw}}$, $Q_{\mathrm{max,cw}}$) and for the PHE using the mixture glycol and water ($Q_{\mathrm{min,gw}}$, $Q_{\mathrm{max,gw}}$). Fig. 9 gives the time evolution of the inlet ($T_{\mathrm{j,i}}$), the outlet ($T_{\mathrm{j,o}}$) jacket temperatures and the jacket set-point temperature ($T_{\mathrm{j,set}}$) computed by the PFCm controller.

Before analyzing the effect of model mismatch we will give the following remarks to demonstrate the performance of the control system using the PFC technique during the stages of heating and cooling of the batch reactor's cycle (ramp set point):

- From Fig. 7 we can notice that the adjusted set-point temperature $T_{\mathrm{d,set}}$ is correctly tracked by the reaction temperature T_{r}.
- Fig. 8 shows a regular evolution of the required thermal flux Q_{cont}. This variable takes a positive value ($Q_{\mathrm{cont}} > Q_{\mathrm{min,er}}$) allowing the use of the electrical resistance and when it becomes negative this allow the use of PHE which use the cold water ($Q_{\mathrm{min,cw}} < Q_{\mathrm{cont}} < Q_{\mathrm{max,cw}}$). We can notice that Q_{cont} plays a real supervisor role because it permits the change of apparatus only when there are an urgent heating or an urgent cooling without provoking deterioration in the tracking of the set-point profile.
- Fig. 9 shows a good regular evolution of the mono-fluid temperatures at the inlet and the outlet of the jacket reactor. We can notice that the jacket set-point temperature $T_{\mathrm{j,set}}$, was tracked correctly by the inlet jacket temperature $T_{\mathrm{j,i}}$ during the heating and the cooling stages.
- The results show the performance of cascade control when there are differences in the dynamics of the different heating/cooling system elements.

We focus now on the effect of the model mismatch on PFC performances during the constant set-point stage. Due to the heat generated by the exothermic reaction, Fig. 7 shows that at the beginning of the feeding (1800 s) the reaction mixture temperature T_{r} overshoots the set-point temperature $T_{\mathrm{d,set}}$ by about 2.5 °C. The control system acts "slowly" and changes apparatus from electrical resistance to PHE which uses the cold water. As shown in Fig. 8, the required thermal flux Q_{cont} becomes negative ($Q_{\mathrm{min,cw}} < Q_{\mathrm{cont}} < Q_{\mathrm{max,cw}}$). This passage takes about 400 s allowing T_{r} to track the set-point temperature after 600 s of the beginning of the feeding time and staying there during all the reaction period with numerous oscillations. Due to the slow action of the control system, at the end of the feeding time T_{r} under-overshoots $T_{\mathrm{d,set}}$ by about 2 °C. Thus, the tracking of the set-point profile at the beginning and the end of the reaction is not entirely satisfactory.

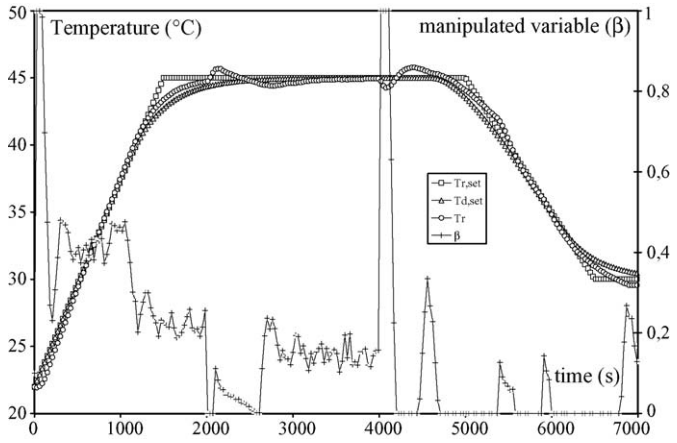

Fig. 10. Temperature and manipulated variable (no-model mismatch).

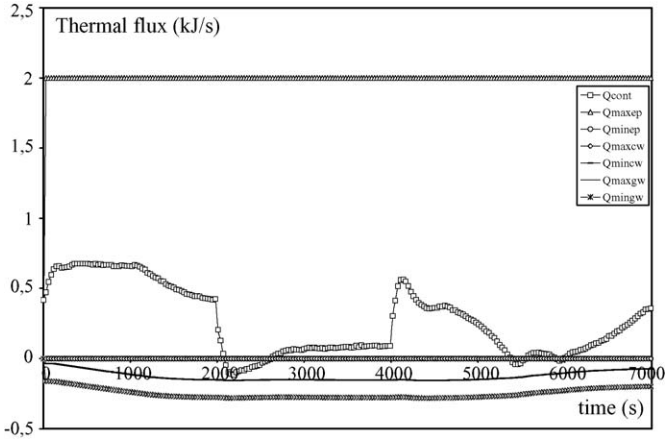

Fig. 11. Limits and required thermal flux (no-model mismatch).

Fig. 8, shows that during the reaction period Q_{cont} oscillates and switches the heating/cooling system between the electrical resistance ($Q_{cont} > Q_{min,ep}$) and the PHE which uses the cold water ($Q_{min,cw} < Q_{cont} < Q_{max,cw}$). The evolution of Q_{cont} is not feasible from the practical point of view and can cause wear and tear of valves and affects the functioning of the different elements of the heating/cooling system.

Fig. 9 shows that the inlet and the outlet jacket temperatures oscillate around 37 °C in order to keep the reactor temperature as close as possible to the set-point.

5.2. Temperature control taking account disturbances due to the exothermic reaction

We have performed an experiment taking into account, in the two internal dynamic models of the controllers PFCs and PFCm, the presence of an exothermic chemical reaction as given by Eqs. (21) and (23). In Eq. (21), Q_{dis}, denotes the disturbance vector which takes account all the heat released. During the heating stage and before the beginning of the reaction, this vector fills up with a zero value and during the reaction period it takes a value of 0.12 (this value is found via simulation). At the end of the reaction and during the cooling stage, this vector fills up again by zero value. In Eq. (23), T_f denotes the feed temperature, equal hold to 20 °C, Q_{rea} denotes the heat released rate, equal hold to $-0.046\,kJ\,s^{-1}$ (this value was found via simulation studies), G_f and G_q denote the steady-state gains related to the feed temperature T_f, and to the released heat Q_{rea} respectively. G_f and G_q take the zero values during the heating stage and before the beginning of the reaction. When the reaction starts, they take a value of 0.5 (this value was found via simulation). At the end of the reaction and during the cooling stage, they take again the zero values.

The reaction was performed between 2000 and 4000 s and the experimental results are presented in Figs. 10–12.

Fig. 10 shows a little overshooting of about 0.3 °C is happened at the beginning of the reaction. The controller PFCs acts "quickly" and changes the thermal element from the electrical resistance to PHE which uses the cold water as shown in Fig. 11. At the same time the inlet jacket set-point temperature $T_{j,set}$ falls quickly from 47 to 37 °C as shown in Fig. 12. The faster response of the control system permits to the reaction mixture temperature T_r to track the set-point temperature $T_{d,set}$ with an under-overshooting of 0.2 °C. After this, PFCs computes a positive value for Q_{cont} in order to use the electrical resistance during all the reaction period with inlet and outlet jacket temperatures evolution about 37 °C. The control system action permits to T_r to track correctly the set-point temperature without oscillations.

At the end of the reaction, $T_{j,set}$ increases quickly from 37 to 51 °C in order to avoid a strong under-overshooting. The slave controller PFCh computes a maximal heating power value ($\beta = 1$) during 100 s (cf. Fig. 10). The mono-fluid temperature increases to 49 °C avoiding a strong under-overshooting (in this case 0.5 °C). After this, the reaction mixture temperature tracks the set-point temperature after an overshooting of 0.9 °C. Thus, tracking of the set-point profile at the beginning and the end of the reaction is entirely satisfactory.

5.3. Discussion

Figs. 13 and 14 show the evolution of the relative control errors $[y_p(i) - y_m(i)]$ between the actual measured reactor temperature and the temperature calculated by the internal models

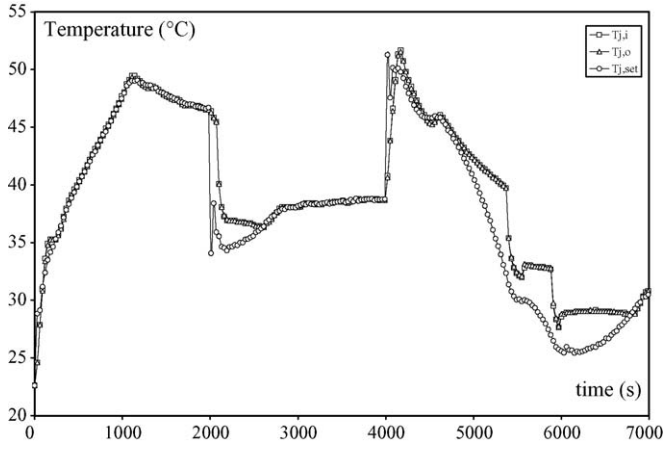

Fig. 12. Inlet, outlet and set-point jacket temperatures (no-model mismatch).

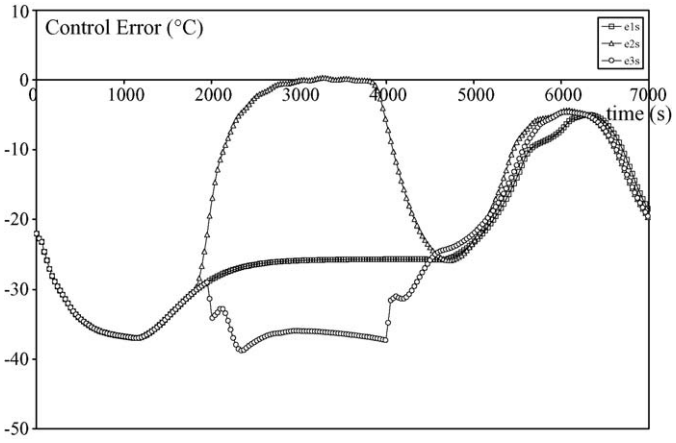

Fig. 13. Relatives control errors evolution: PFCs controller.

used to design PFCs and PFCm controllers, respectively. In Figs. 13 and 14, e_{1s} and e_{1m} are the two control errors that permit a good set-point tracking in the absence of disturbances and they are plotted here for comparison purpose. e_{2s} and e_{2m} are the control errors for the model mismatch case and they are calculated using internal models (30) and (31) respectively. Finally (e_{3s}) and (e_{3m}) are the control errors for the no-model mismatch case and they are calculated using internal models (21) and (23), respectively. Figs. 13 and 14 indicate that during the reaction period, e_{2s} and e_{2m} evolve very far from e_{1s} and e_{1m}, respectively, contrary to e_{3s} and e_{3m} that evolve very close to these errors. Due to the release of heat, control errors e_{2s} and e_{2m} persist and push PFCs and PFCm controllers to calculate a positive and a negative values for Q_{cont} and a higher and a lower values for $T_{j,set}$ in order to track the set-point temperature profile ($T_{d,set}$). This is traduced by a numerous oscillations of the manipulated variable (β) (cf. Fig. 7), the required thermal flux (Q_{cont}) (cf. Fig. 8) and the jacket set-point temperature ($T_{j,set}$) (cf. Fig. 9). The evolution of control errors e_{3s} and e_{3m} shows that at least an adequate model for the batch reactor permits a better temperature control.

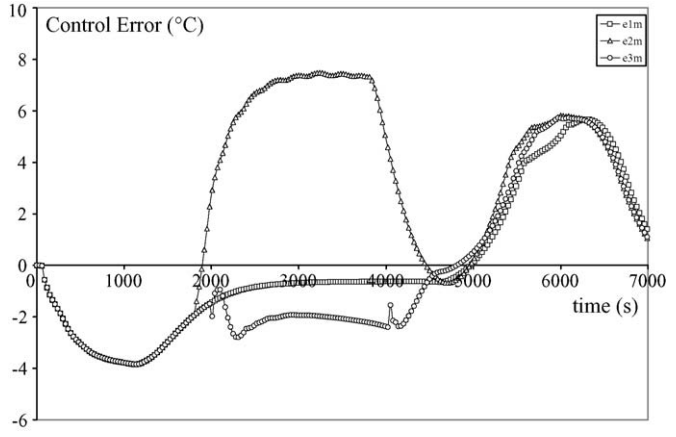

Fig. 14. Relatives control errors evolution: PFCm controller.

6. Conclusions

In this paper, the performance of the PFC technique with regard to the temperature control of pilot-plant batch reactor equipped with a mono-fluid heating/cooling system was performed. It turned out that at least good basic modeling of the process is necessary. This could be shown by the example of an exothermic reaction. As heat released by a chemical reaction was not considered in the internal controller model – even if the PFC reacted correctly – the controller cannot anticipate the heat released which results in an unsatisfactory performance. When the heat released by the chemical reaction was considered, the control system can anticipate the disturbance caused and permits a better tracking of the set-point temperature profile. Thus the choice of the internal model is of crucial importance for PFC, since the capacity of prediction constitutes the base of all the specifications of performance. However, it is necessary to know the parameters related to the reaction with a certain degree of accuracy. Even if the batch reactor must remain polyvalent, the reactions were generally subjected to a certain number of studies. Thus, one can consider having a sufficient knowledge of those to adjust the parameters. Simulation studies have shown that at least 25% of knowledge about the heat released by the reaction can avoids a strong over-shooting at the beginning of the reaction period (Bouhenchir, 2000).

Otherwise, experimental results show that the PFC technique enables a precise tracking of the set-point temperature profile, and also the performance of the cascade control was proved when there are differences in dynamics of the different thermal elements.

Considering these results it can be summarized that PFC control provides high flexibility and robustness in combination with precise tracking of set-point profiles. Therefore PFC technique can be considerate as an appropriate solution for the temperature control of batch reactors, and the developed control strategy can be implemented to control industrials batch reactors. In this case, preliminary identification of the model's parameters is required.

Acknowledgement

The authors would like to acknowledge the productive discussion with Jacque Richalet that enabled us to accomplish this work.

Appendix A

A.1. Docking procedure

Starting from t_1 ($t_1 < t_{f1}$), the set-point temperature profile will follow an exponential function. This function should be chosen so that the adjusted set-point profile will be continuous and its final value will be equal to the original set-point profile.

A.1.1. Increasing ramp

The adjusted set-point temperature profile and the original set-point temperature profile for an increasing ramp are plotted

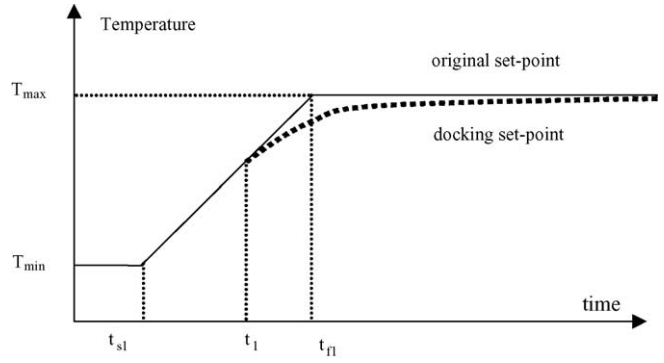

Fig. A1. Docking procedure: increasing ramp.

in Fig. A1. Eq. (A1) gives a mathematical formulation of the adjusted set-point temperature profile $T_{d,set}$.

$$T_{d,set}(t) = T_{min} \quad t \le t_{s1},$$
$$T_{d,set}(t) = T_{min} + \frac{T_{max} - T_{min}}{t_{f1} - t_{s1}}(t - t_{s1}) \quad t_{s1} < t \le t_1,$$
$$T_{d,set}(t) = T_{max} - (T_{max} - T_{d,set}(t_1)) \exp\left(\frac{t_1 - t}{t_{f1} - t_1}\right) \quad t > t_1. \tag{A1}$$

The choice of t_1 it is a kind of compromise between overshooting and deviation from the original set-point.

A.1.2. Decreasing ramp

The adjusted set-point temperature profile and the original set-point temperature profile for a decreasing ramp are plotted in Fig. A2. From the time t_{12}, the set-point temperature profile will be composed by two different exponential functions:

- The first one defines the adjusted set-point profile between time t_{12} et t_2.
- The second one, starts from t_2. At t_2, the two functions should be equal.

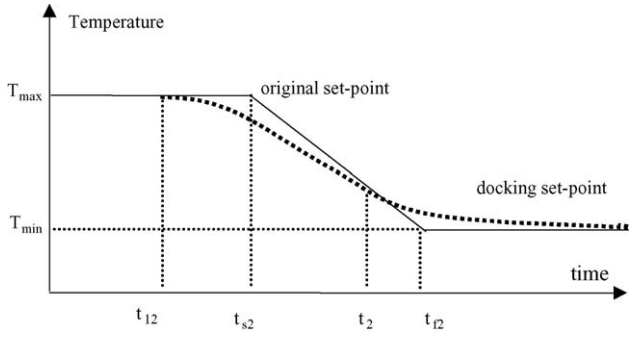

Fig. A2. Docking procedure: decreasing ramp.

The adjusted set-point temperature profile is given by the following equation:

$$T_{d,set}(t) = T_{max} \quad t \le t_{12},$$
$$T_{d,set}(t) = T_{max} - C_1 \{(t - t_{12}) - (t_{s2} - t_{12}) \times \left[1 - \exp\left(\frac{t_{12} - t}{t_{s2} - t_{12}}\right)\right]\} \quad t_{12} < t \le t_2,$$
$$T_{d,set}(t) = T_{min} + (T_{d,set}(t_2) - T_{min}) \times \exp\left[C_2\left(\frac{t - t_2}{T_{d,set}(t_2) - T_{min}}\right)\right] \quad t > t_2 \tag{A2}$$

where $C_1 = (T_{max} - T_{min}/t_{f2} - t_{s2})$ and $C_2 = C_1[\exp(t_1 - t_2/t_{s2} - t_1) - 1]$.

The choice of t_{12} it is a kind of compromise between overshooting and deviation from the original set-point.

References

Badgwell, T. A., & Qin, S. J. (2001). Review of non-linear model predictive control applications. In B. Kouvaritakis, & M. Cannon (Eds.), *Nonlinear predictive control: theory and practice* (pp. 3–32), IEE Control Engineering series 61.

Baltussen, E. M. P. B., (1995). Thermal control of chemical batch reactors with predictive functional control. Master Thesis. University of Delft.

Boucher, P., & Dumur, D. (1996). *la commande prédictive*. Paris: Technip.

Bouhenchir, H., (2000). Mise en œuvre de la commande prédictive pour la conduite thermique d'un réacteur discontinu équipé d'un système monofluide. PhD thesis. Toulouse: Institut National Polytechnique.

Bouhenchir, H., Cabassud, M., Le Lann, M. V., & Casamatta, G. (2000). A heating/cooling management to improve controllability of batch reactor equipped with a mono-fluid heating/cooling system. In *European Symposium on Computer Aided Process Engineering – 10 (Florence – Italy). Sauro pierucci* (pp. 601–606).

Bouhenchir, H., Cabassud, M., Le Lann, M. V., & Casamatta, G. (2001). A general simulation model and a heating–cooling strategy to improve controllability of batch reactors. *Trans IchemE, Part A*, *79*, 641–654.

Defaye, G., Régnier, N., Chabanon, J., Caralp, L., & Vidal, C. (1993). Adaptive predictive temperature control of semi-batch reactors. *Chemical Engineering Science*, *48*(19), 3373–3382.

Friedrich, M., & Perne, R. (1995). Design and control of batch reactors: an industrial viewpoint. *Computers and Chemical Engineering*, *19*, S357–S368.

Huzmezan, M., Gough, B., & Kovac, S. (2002). Advanced control of batch reactor temperature. In *World Batch Forum North American Conference*.

Juba, M. R., & Hamer, J. W. (1986). Progress and challenges in batch process control. In *Proceedings of the CPC III. CACHE*.

Le Lann, M. V., Cabassud, M., & Casamatta, G. (1995). In R. Berber (Ed.), *Adaptive model predictive control, methods of model based process control* (pp. 426–458). Dordrecht: Kluwer Academic Publishers.

Lee, K. S., Chin, I. S., & Lee, H. J. (1999). Model predictive control technique combined with iterative learning for batch processes. *AIChE Journal*, *45*(10), 2175–2187.

Özkan, G., Hapoglu, H., & Alpbaz, M. (1998). Generalized predictive control of optimal temperature profiles in a polystyrene polymerization reactor. *Chemical Engineering Proceedings*, *37*, 125–139.

Peebles, S. M., Hunter, S. R., & Corripio, A. B. (1994). Implementation of a dynamically-compensated PID control algorithm. *Computers and Chemical Engineering*, *18*, 995–1000.

Preuß, K., Le Lann, M. V., & Anne-Archard, G. (2000). Supervisory temperature control of batch reactors: Application to industrial plant, vol. 1. In *ADCHEM 2000* (pp. 225–230) (Preprints).

Preuß, K., Le Lann, M. V., Cabassud, M., Richalet, J., & Casamatta, G. (1998). Thermal control of chemical batch reactors with predictive functional control. *Journal a*, *39*(4), 13–20.

Primucci, M., & Basualdo, M. (2002). Thermodynamic predictive functional control applied to CSTR with jacket system. In *Proceedings of the IFAC 15th Triennial World Congress*.

Qin, S. J., & Badgwell, T. A. (1996). An overview of Industrial Model Predictive Control Technology. In *Proceedings of the CPC-V Tahoe* (pp. 232–256).

Richalet, J. (1993). *Pratique de la commande prédictive*. Paris: Hermes.

Richalet, J., Lavilelle, G., & Mallet, J. (2004). *La commande prédictive: mise en œuvre et applications industrielles*. Eyrolles.

Rivera, D. E., & Gaikwad, S. V. (1996). Digital PID controller design using ARX estimation. *Computers and Chemical Engineering*, *20*, 1317–1334.

Rodrigues, J. A. D., Toledo, E. C. V., & Maciel Filho, R. (2002). A tuned approach of predictive and adaptive GPC controller applied to fed-batch bioreactor using complete factorial design. *Computers and Chemical Engineering*, *26*, 1493–1500.

Xaumier, F., Le Lann, M. V., Cabassud, M., & Casamatta, G. (2002). Experimental application of nonlinear model predictive control: temperature of an industrial semi-batch pilot plant-reactor. *Journal of Process Control*, *12*, 687–693.